SSCL-Preprint-273

SSCL-Preprint-273
May 1993
Distribution Category: 414

D. Anderson
L. Schneider

# Design and Preliminary Testing of the LEB Extraction Kicker Magnet at the SSC

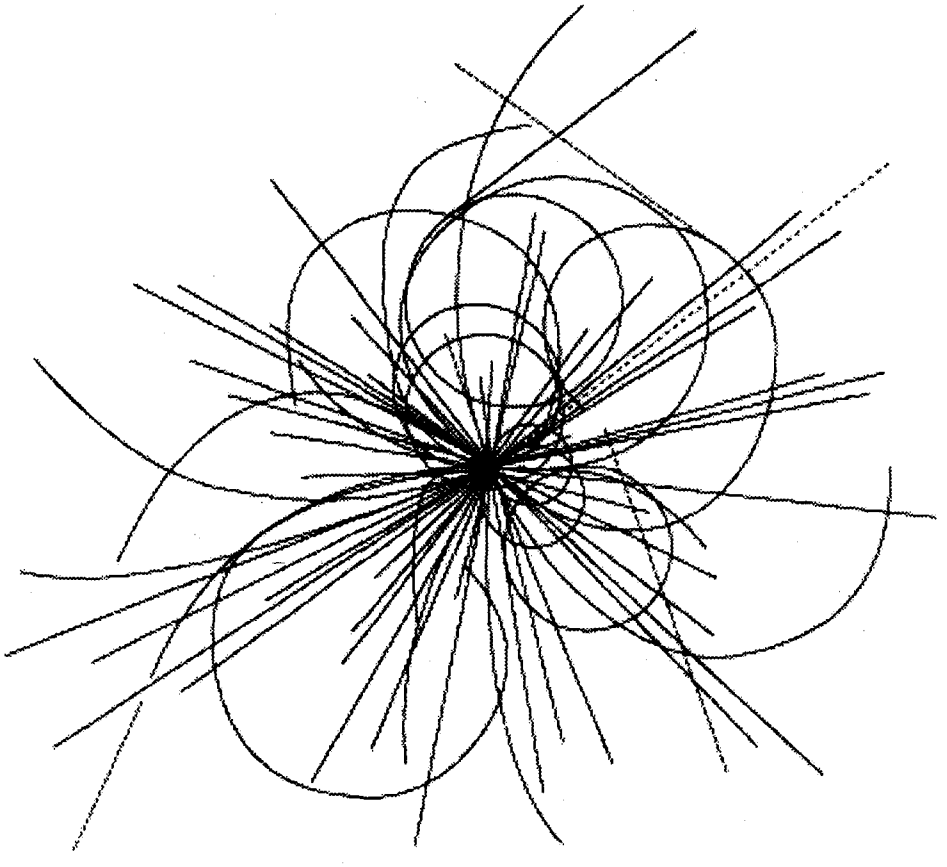

## Superconducting Super Collider Laboratory

SSCL-Preprint-273

# Design and Preliminary Testing of the LEB Extraction Kicker Magnet at the SSC*

D. Anderson and L. Schneider

Superconducting Super Collider Laboratory†
2550 Beckleymeade Ave.
Dallas, TX 75237

May 1993

*To be presented at the 1993 IEEE Particle Accelerator Conference on May 17–20, Washington, D.C.
†Operated by the Universities Research Association, Inc., for the U.S. Department of Energy under Contract No. DE-AC35-89ER40486.

# Design and Preliminary Testing of the LEB Extraction Kicker Magnet at the SSC

D. E. Anderson and L. X. Schneider
Superconducting Super Collider Laboratory*
2550 Beckleymeade Ave., Dallas, TX 75237 USA

*Abstract*

The kicker magnet for extracting beam out of the Low Energy Booster is required to generate an integrated field of 0.06 T-m for 2 μs, rising from 1% to 99% of peak in ≤80 ns. Technologies for pulsed magnets of this variety, along with the engineering trade-offs of each, will be presented. Details of the electrical design of a vacuum-insulated 25-Ω travelling-wave (TW) kicker magnet, with a 5 × 7 cm ferrite aperture, will be discussed. The results of low-voltage tests of the prototype TW magnet and a solid-core design will also be presented. Application of experimental data and design theory to the final magnet design will be mentioned.

## I. INTRODUCTION

The Low Energy Booster (LEB) at the Superconducting Super Collider (SSC) is designed to accelerate protons to momentum of 12 GeV/c. In order to steer the beam upon extraction into the septum magnets, a vertical angular deflection of 1.5 mrad is required. Table 1 summarizes the LEB Extraction kicker magnet requirements.

Table 1
LEBE Kicker Magnet Requirements Extraction

| | |
|---|---|
| Nominal ∫ B·dl | 0.06 T-m |
| ΔB/B Temporal | ≤±1% |
| ∫ B·dl Risetime | ≤80 ns (1–99%) |
| ∫ B·dl Pulsewidth | 2 μs |
| ∫ B·dl Falltime | ≤50 ms (99–1%) |
| Aperture | 5 H × 7 V cm |
| Good Field Region (GFR) | 2 H × 4 V cm |
| GFR "Kick" Uniformity | ≤5% |

Kicker magnet design has historically taken two approaches, depending on the magnets' performance requirements. The more common approach utilizes a lumped section of C-shaped ferrite or magnetic steel cores, energized by a conductor passing through the cores' aperture. The other technique, used for faster risetime requirements, divides the C-cores into discrete sections to form a uniform impedance transmission line. The sections are capacitively coupled to the return conductor through a series of capacitive plates or discrete capacitors.

*Operated by the Universities Research Association, Inc., for the U.S. Department of Energy under Contract No. DE-AC35-89ER40486.

Prototype magnets of the two varieties discussed above were built and tested at the SSC Laboratory. A 25-Ω "travelling wave" TW magnet utilizing 28 or 25 cells was designed [1] with 25.1-mm cell lengths. Figure 1 shows a cutaway view of this magnet. A "solid core" (SC) magnet was also built to compare against the TW variety and to establish a database for future systems.

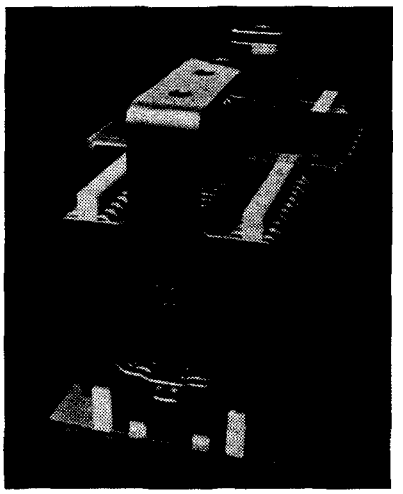

Figure 1. Cutaway view of the 28-Cell LEB extraction TW kicker magnet.

## II. TW MAGNET DESIGN

### A. Inductance Calculations

A first-order approximation of the inductance can be made from the following simple formula, which assumes that all of the magnetic energy is contained in the airgap and that the field is uniform throughout the gap:

$$\frac{L}{l} = \mu_0 \frac{W}{g},$$

where $W$ is the width of the airgap and $g$ is the gap length. For a 5 × 7-cm gap, this becomes 1760 nH/m. The magnet geometry was simulated using Maxwell2D (Ansoft Corporation) to account for fringe magnetic and electric field effects. The **B·H** product was integrated over the magnetic region to determine the magnet's inductance per unit length. The result was 2123.2 nH/m, giving a resultant cell inductance of 2123.2 nH/m × 0.0251 m/cell = 53.3 nH. The formula yields a low value since it does not account for fringing fields and energy contained in the ferrite. Figure 2 shows the Maxwell2D plot of the equal magnetic vector potential lines with $\mu_r = 300$, the approximate value at the frequencies present in the risetime of the pulse. Electric field vectors, which also produce undesirable qE forces on the beam, are also shown.

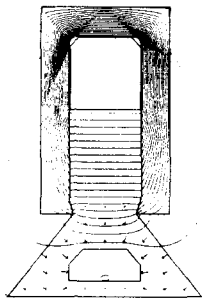

Figure 2. Maxwell2D Plot of LEBE extraction prototype magnet flux lines and electric field vectors.

*B. Capacitance Calculations*

Knowing the cell inductance and the desired magnet impedance, the cell capacitance can be calculated from the formula $C_{cell} = L_{cell} / Z_0^2 = 85.3$ pF. Capacitance is developed by interleaving aluminum plates that connect to the busbar and return conductor to produce an overlap area *A*. The capacitance of this geometry is given by:

$$C_{cell} = 2\frac{A\varepsilon_0}{d} + 2C_{fr},$$

where *d* is the plate spacing and $C_{fr}$ is the fringing effect from the edges of the plates. The fringing term can be approximated as 10 pF per linear meter of plate edge [2]. From this equation, an estimated overlap area of 204 $cm^2$ was indicated to achieve the desired capacitance and magnet impedance.

*C. Electrical Length*

It can be shown that for a first order approximation, the risetime of the integrated field is the sum of the electrical length of the magnet and the current risetime of the input pulse. A pulse generator has been built at the SSC that is designed to produce a voltage pulse risetime into 12.5 Ω of 20 ns (10–90%)[3]. This sets the maximum electrical length of the magnet to approximately 60 ns.

The electrical length of a TW magnet cell can be approximated as $(L_{cell}C_{cell})^{1/2}$, or 2.13 ns for this design. Dividing this into the maximum electrical length, the maximum number of cells is found to be 28. The prototype magnet was designed to accommodate fewer cells in the event actual cell parameters varied significantly from design calculations.

*D. Other Magnetic Calculations*

Three other important parameters were derived from the Maxwell2D simulations. The magnetic "gain," which defines the flux density achievable per unit of current, was found to be 22.6 μT/A in the center of the airgap. At 580 A, a flux density of 0.0131 T is achievable, allowing 110% of the $|\int B\cdot dl|$ specification to be met with 8 TW magnets 25 cells long. The variation of the flux density over the area enclosed within the "good field region" was found to the within ±0.95% of nominal. The total variation for a magnet operating at 580 A and 14.5 kV, including electric field contributions, is +1.2–0.3% of nominal in the same region. Finally, the maximum flux density in the ferrite was found to be $2.62 \times 10^{-4}$ T/A, giving a maximum flux density in the ferrite of 0.151 T at the expected operating current of 580A. For the CMD5005 ferrite used in this application, the saturation flux density is 0.33 T at 25°C.

*E. SPICE Simulations of Magnet Performance*

The cells of the TW kicker magnet were modelled using an equivalent T-section circuit model [1]. The $L_1$ term, arising from mutual coupling between cells and self-inductance of the capacitor plates, was calculated to be about 70 nH from Grover's formula [4] scaled to the CERN FAK magnet data [2]. A 25-cell TW magnet was then simulated using SPICE, with the results shown in Figure 3. From this, an $\int B\cdot dl$ signal 1–99% risetime of 73.8 ns is predicted, and ΔB/B varies by ±0.55%.

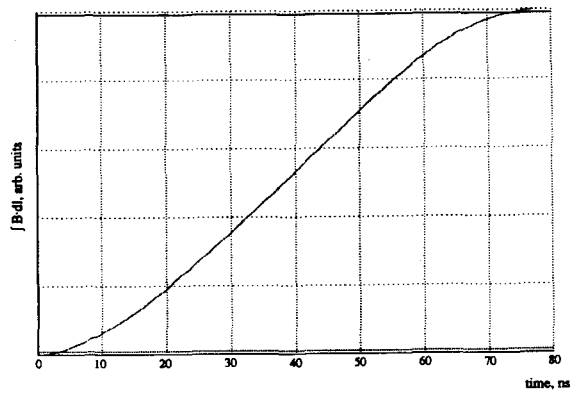


Figure 3. SPICE simulation of magnet performance.

## III. EXPERIMENTAL RESULTS

*A. Experimental Setup and Probes*

An HP 8082A variable rise and falltime 5-V, 50-Ω pulser, with a 50-to-25-Ω impedance-matching network, was used to pulse the magnet in the majority of the experiments. Where greater signal levels were required, a Spi-Pulse 25-reed switch pulser with 115 ns of charged cable was used to drive the magnet up to 40 A. Digitizers included a Tektronix 11403 with a 11A34 amplifier for repetitive signals and an HP 54510A for single-shot signals.

B-dot probes were fabricated using printed circuit board technology. Spot probes consisted of a circular "wire" trace with an area of 9.57 $mm^2$, coupled to the scope via RG-405 semirigid coaxial cable. $\int B\cdot dl$ probes were designed using an exponentially tapered strip mounted on a G-10 substrate. The taper should provide a high-bandwidth match at both the scope input end and the shorted end. Due to the significant capacitive coupling between the $\int B\cdot dl$ probe and the magnet, the signal produced when the probe was right-side-up was subtracted from the signal produced when the probe was inverted. Furthermore, to minimize errors resulting from the direction of wave propagation in the probe relative to the magnet, responses from the two probe orientations were averaged [2], [5].

*B. Travelling Wave Magnet Results*

A 25-and 28-cell TW magnet were constructed and compared. When pulsed with a 10–90% voltage risetime of 20 ns (1–99% ~55 ns), the $\int B\cdot dl$ 1–99% risetimes were 78.4 and

84.0 ns, respectively. The difference between the measured and simulated risetime was primarily due to subtle differences in the simulated and actual input waveforms.

The 28-cell magnet's total inductance and capacitance were measured using an HP 4284A Precision LCR Meter. At 1 MHz, an inductance of 1927.6 nH and a capacitance of 3315.1 pF were measured. Dividing by the number of cells and correcting for end effects, these numbers scale to $L_{cell} = 66.4$ nH and $C_{cell} = 92.7$ pF. The cell inductance is about 25% higher than that predicted by Maxwell2D, probably attributable to cell-to-cell mutual coupling. The capacitance is very close to that predicted by simple formulas, and can be corrected for fringe field effects by using $C_{fr} = 11$ pF/(linear m).

Another technique was used to determine cell inductance by measuring the propagating cell voltages. From this, the cell inductance can be calculated as $\tau^2/C_{cell}$, where $\tau$ is the propagation delay through a given cell. For an average cell propagation time of 2.38 ns, a cell inductance of 61 nH is calculated. Figure 4 shows the measured voltages for the first 8 cells.

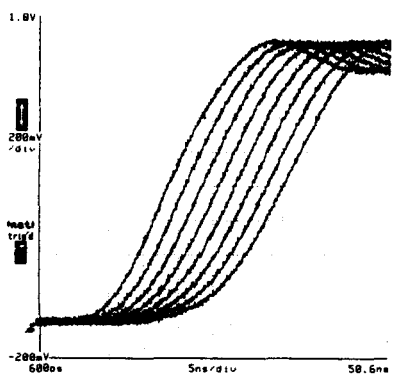


Figure 4. Measured cell voltages for the first 8 cells.

Using an HP 8751A Network Analyzer, the cutoff frequency was measured to be approximately 50 MHz. From this and the $L_{cell}$ and $C_{cell}$ values measured, an $L_1$ term for the T-section model of 100 nH can be calculated.

*C. Solid-Core Magnet Results*

A solid-core magnet was constructed by placing a variable number of 20-mm-long ferrite cores in an aluminum enclosure designed to fit tightly around the cores. A busbar of dimensions identical to the TW magnet was then routed through the ferrite pieces. Inductances and other magnetic parameters were therefore similar to those in the TW magnet. Varying voltage risetimes from a 25-Ω system were pulsed into the magnet, for various numbers of ferrite cores, and the integrated flux density risetime was measured. Figure 5 graphs the results of this experiment.

To improve risetime performance, the solid-core magnet was compensated with discrete capacitors at various locations along its length. By introducing gaps between ferrite units and inserting discrete capacitors, a lumped N-section transmission line was produced. Values for N = 1, 2, and 3 were tested. A 25-ferrite core magnet, grouped into sections of 9, 8, and 8 20-mm ferrite cores, with corresponding compensation

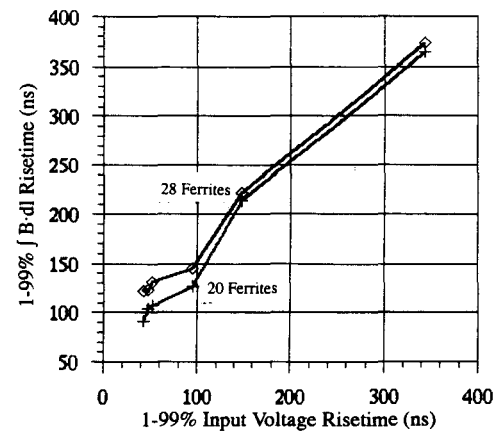


Figure 5. Solid-core magnet response.

capacitance values of 100, 200, and 440 pF, was constructed and tuned empirically. When pulsed with a voltage with a 10–90% risetime of 20 ns, the 1–99% ∫ B·dl risetime was found to be ~70 ns, while ΔB/B remained within the ±1% flattop tolerance. This risetime is better than that measured for a TW magnet of an identical number of ferrite cores, probably due to the lack of inter-ferrite fringing fields, lower overall capacitance and inductance, and lower stray inductance of the discrete capacitors. However, the applicability of these results to a higher-current, high-voltage version of this magnet is questionable. Higher field magnitudes may lead to additional dispersion and/or other effects, thereby further degrading the magnet's performance.

## IV. CONCLUSION

Although a complex structure, the TW magnet can be accurately modelled using a few simple formulas and simulation tools, with prediction of pertinent parameters to within ~10% or better. Experimental results confirm the TW magnet design, and indicate the need for further investigations into the behavior of capacitively-compensated solid core magnets. The encouraging solid-core magnet results, if applicable under high-voltage conditions, will substantially reduce the complexity and cost of kicker magnets requiring risetimes under 100 ns.

## V. REFERENCES


[1] D. Fiander, "A Review of the Kicker Magnet Systems of the PS Complex," *Conference Record of the 12th National Particle Accelerator Conference* (Moscow, 1990).

[2] Private conversation with D. Fiander, 12/91.

[3] G. Pappas & D. Askew, "Preliminary Testing of the LEB to MEB Transfer Kicker Modulator Prototype," presented at this conference.

[4] Grover, *Inductance Calculations*, p. 35 (Dover, NY, 1946).

[5] G. Nassibian, "Travelling Wave Kicker Magnet with Sharp Rise and Less Overshoot," *IEEE Trans. on Nuc. Sci.*, Vol. NS-**26**, June 1979, pp. 4018–20.